ACS Medicinal Chemistry Letters

Letter

pubs.acs.org/acsmedchemlett

Cyclic RGD Peptides Incorporating Cycloalkanes: Synthesis and Evaluation as PET Radiotracers for Tumor Imaging

Ji-Ae Park,[†] Yong Jin Lee,[†] Ji Woong Lee,[†] Kyo Chul Lee,[†] Gwang il An,[†] Kyeong Min Kim,[†] Byung il Kim,[‡] Tae-Jeong Kim,*[,§] and Jung Young Kim*[,†]

[†]Molecular Imaging Research Center, Korea Institute of Radiological and Medical Sciences, Seoul 139-706, Republic of Korea

[‡]Department of Nuclear Medicine, Korea Institute of Radiological and Medical Sciences, Seoul 139-706, Republic of Korea

[§]Institute of Biomedical Engineering Research, Medical School, Kyungpook National University, Daegu 702-701, Republic of Korea

Supporting Information

ABSTRACT: Two new bicyclic arginine-glycine-aspartic acid (RGD) peptides, c(RGD-ACP-K) (**1a**) and c(RGD-ACH-K) (**1b**), incorporating the aminocyclopentane (ACP) and aminocyclohexane (ACH) carboxylic acids, respectively, were synthesized by grafting the aminocycloalkane carboxylic acids onto the tetrapeptide RGDK sequence. These peptides and their conjugates with DO3A (1,4,7,10-tetraazacyclododecane-1,4,7-trisacetic acid) (**2a**–**b**) exhibit high affinity toward U87MG glioblastoma cells. Their affinity is greater than that exhibited by c(RGDyK). Labeling these conjugates with radiometal ^{64}Cu resulted in high radiochemical yields (>97%) of the corresponding complexes, abbreviated as c(RGD-ACP-K)-DOTA-^{64}Cu (**3a**) and c(RGD-ACH-K)-DOTA-^{64}Cu (**3b**). Both **3a** and **3b** are stable for 24 h in human and mouse serums and show high tumor uptake, as observed by positron emission tomography (PET). Blocking experiments with **3a** and **3b** by preinjection of c(RGDyK) confirmed their target specificity and demonstrated their promise as PET radiotracers for imaging $\alpha_v\beta_3$-positive tumors.

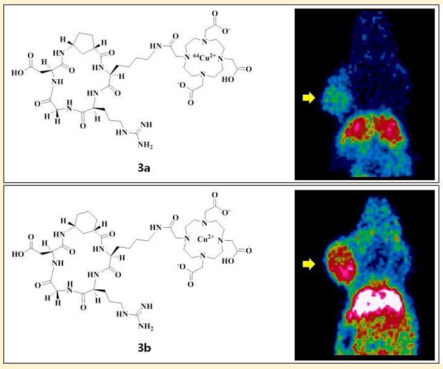

KEYWORDS: *Cyclic RGD peptides, integrin receptor, radiotracers, PET, tumor targeting*

Arginine-glycine-aspartic acid (RGD) binds to the $\alpha_v\beta_3$ and $\alpha_v\beta_5$ integrins that are overexpressed in nascent endothelial cells during angiogenesis in various tumors, and yet not in inactive endothelial cells.[1,2] To detect tumor cells in their early stages, it is essential to deliver tumor-targeting peptides, such as RGDs, incorporated into imaging probes.[3,4] A wide range of imaging probes in the form of bifunctional chelates (BFCAs) are used in various diagnostic techniques, including positron emission tomography (PET), single photon emission computed tomography (SPECT), and magnetic resonance imaging (MRI).[5,6]

Consequently, a great number of RGD derivatives have been developed in an effort to improve the pharmacokinetics and binding affinity toward specific cell surface receptors.[7] Early studies demonstrated that simple linear RGD peptides are active against several integrins but lack selectivity.[8,9] Head-to-tail cyclization of RGD peptides increases both the binding affinity and selectivity of $\alpha_v\beta_3$ and $\alpha_v\beta_5$ integrins.[10,11] Examples include cyclic peptides such as c(RGDfK), c(RGDyK), RGD4C, and RGD10 (see Chart S1, Supporting Information). Specifically, c(RGDfK) and c(RGDyK) have been widely employed in tumor targeting.[12] Quite naturally, binding affinity increases with an increase in the number of c(RGD) moieties. For instance, multimeric c(RGD) systems are found in dendrimers and nanoparticles.[13,14] One drawback of multimeric c(RGD) systems is that they often exhibit a low tumor/blood ratio because of high uptake in normal organs.[15,16] Another approach to increase receptor affinity and selectivity is the development of "bicyclic peptides". Bicyclic peptides are that a cyclic peptide incorporates an additional ring moiety within the cycle.[17−20] Casiraghi demonstrated that a series of bicyclic RGD peptides, formed by grafting aminocyclopentane carboxylic acids (Acpca) into the cyclic RGD tripeptide sequence, possess significantly increased affinity.[21,22] Hao recently reported the cyclization of linear RGD with BFCA, leading to the formation of a different type of bicyclic RGD peptides for imaging integrins.[17] In contrast to the multimeric peptides mentioned above, these bicyclic systems employ single c(RGD) and have demonstrated rapid blood clearance with an adequate tumor/blood ratio.[8] Bicyclics are straightforward to synthesize, modify, and use in therapy as well as diagnosis.

Motivated by the observations that bicyclic c(RGD) peptides put a new entry into highly efficient BFCAs for use in PET radioimaging, we report the synthesis of two bicyclic c(RGD) peptides **1a**–**b** and their DO3A conjugates **2a**–**b**. Radiolabeling with radiometal ^{64}Cu ($t_{1/2}$ = 12.7 h; β^+ 19%, EC 41%)[23] results

Received: April 2, 2014
Accepted: July 10, 2014
Published: July 10, 2014

in the formation of **3a**–**b**. One characteristic of **1** is that it adopts a tetrapeptide (RGDK) platform, whereas Casiraghi's system employs a tripeptide (RGD) framework. In **1b**, a cyclohexane moiety is grafted onto the bicycle for comparative studies. ^{64}Cu-labeled bicyclic RGD peptides are rarely used as PET radiotracers *in vivo*.[17] ^{64}Cu-labeling is more convenient than ^{18}F-labeling because it does not require multistep syntheses, such as those necessary for [^{18}F]galacto-RGD and [^{18}F]AH111585.[24−27]

Scheme 1 shows the synthesis of **1**, **2**, and **3**. Bicyclic peptides (**1a**–**b**) and their conjugates with DO3A (**2a**–**b**) were

Scheme 1. Synthesis of 1, 2, and 3

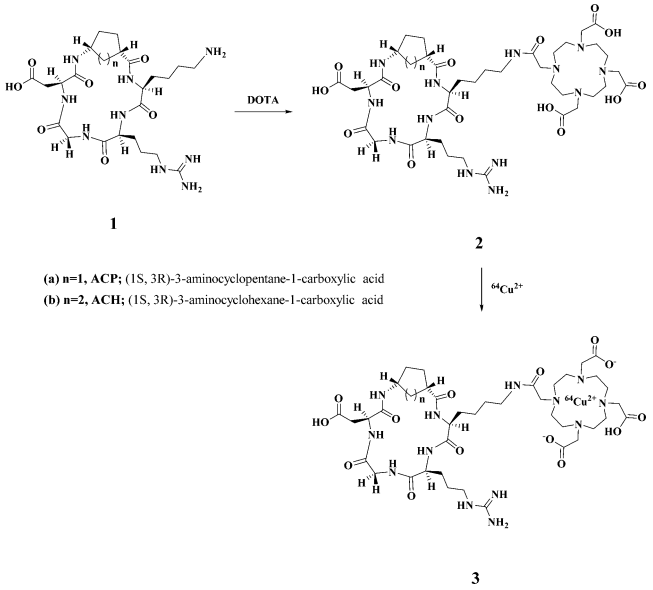

prepared in high yields following conventional SPPS.[28] By inserting L-lysine (K) in the bicycle, it can be conjugated with various bifunctional chelates such as DOTA, NOTA, and NODAGA.[3,6,26,27] Product formation was confirmed by MALDI-mass spectroscopy, and the chemical purity of **2** was greater than 95%, as confirmed by HPLC. Radiolabeling of **2** with ^{64}Cu resulted in high yields of corresponding complexes (**3**). Both the radiochemical yields and purities were greater than 98% as confirmed by radio-TLC.

The chemical equivalence of **3b** with its natural analogue c(RGD-ACH-K)-DOTA-^{nat}Cu, was established by analytical HPLC chromatography (Figure 1). c(RGD-ACH-K)-DOTA-^{nat}Cu and **3b** demonstrated similar retention times (R_t) of 11.6 and 12 min, respectively. The specific activities of **3a**

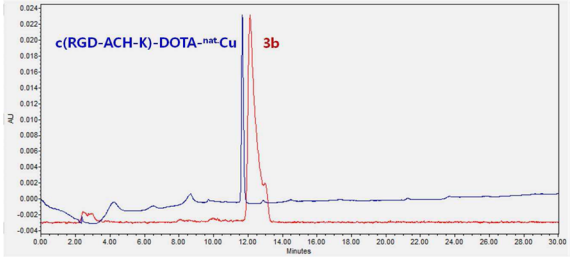

Figure 1. Analytical HPLC chromatograms of c(RGD-ACH-K)-DOTA-^{nat}Cu (blue, 254 nm) and **3b** (red, γ trace).

and **3b** after labeling (n = 10) were 22.9 ± 0.7 and 22.7 ± 0.8 Ci/g.

Except for **2b**, all compounds demonstrated high affinity toward the $\alpha_v\beta_3$ integrin receptor in U87MG glioblastoma cells. Their affinities were better than that of (RGDyK). The IC_{50} values for **1a**, **1b**, **2a**, **2b**, and c(RGDyK) against ^{125}I-echistatin were 3.5 ± 0.7, 13.2 ± 2.2, 15.7 ± 1.6, 61.1 ± 9.5, and 17.1 ± 1.4 nM, respectively (Figure 2). The IC_{50} of **1a** is nearly four

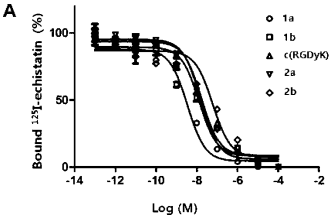

B

Compound	IC_{50} (nM)
c(RGDyK)	17.1 ± 1.4
1a	3.5 ± 0.7
1b	13.2 ± 2.2
2a	15.7 ± 1.6
2b	61.1 ± 9.5

Figure 2. Cell binding assay of RGD peptides in U87MG cells (A); IC_{50} values (average of 3 measurements plus the standard deviation) of each RGD compound (B).

times as high as that of **1b**. This difference may be explained by the difference in conformational rigidity (or strain) between the aminocyclopentane derivative (**1a**) and the aminocyclohexane analogue (**1b**). As mentioned in introduction, it is well-known that the binding affinities of cyclic RGD peptides depend on the stereochemistry of the individual amino acids and the conformation of the overall cyclic backbone.[8,21,22] The literature has described the conformational effect as follows: (i) A cyclic peptide is more effective than its linear counterpart; (ii) a bicyclic structure incorporating a cyclic linker in the cyclic backbone is more effective than a simple cyclic RGD; (iii) the smaller the ring size of the incorporated cyclic moiety, the higher the binding affinity. Non-natural analogues are known to exhibit higher affinity than natural amino acids.[21,22] On the basis of these observations, the cyclohexane moiety present in **1b** and **2b** should exhibit greater conformational flexibility than the cyclopentane moiety in **1a** and **2a**.[29] The binding affinity of **1** should be higher than that of c(RGDyK) because **1** contains non-natural amino acids with cycloalkane groups. The apparent lower binding affinity of **2** relative to **1** can be explained by conjugation of DO3A as a BFCA. Consequently, the slow metabolism *in vivo* of **3a** compared with the corresponding complex of natural c(RGDyK) may be explained by the stereochemistry cited above.[30,31]

Complex **3** showed little radiochemical degradation (radiochemical purity > 97%) according to the radio-TLC analysis performed in human and mouse serums for 24 h (Table S1, Supporting Information). Both **3a** and **3b** are highly soluble in water and have log P values of −4.22 ± 0.09 and −4.41 ± 0.05, respectively (note that the log P for c(RGDyK)-DOTA-^{64}Cu is −2.8 ± 0.04).[32] The differences in hydrophilicity may be reflected in the biodistribution patterns. Tables S2 and S3, Supporting Information, list the tissue distribution profiles for **3a** and **3b**, in nude mice with U87MG glioblastoma tumors.

Figure 3 shows the detailed biodistribution patterns in the blood, kidneys, liver, and tumor. Both compounds are excreted rapidly at almost identical rates in the blood and kidney, while the excretion rates in the liver and tumor differ as a function of time. The liver-uptake of **3a** is slightly higher than that of **3b** at 30 min p.i. and decreases over time. The uptake of **3b** increases to a maximum (3.49 ± 0.92 %ID/g) at 3 h p.i. and then decreases to eventually match the uptake of **3a** at 18 h p.i. The

dx.doi.org/10.1021/ml500135t | ACS Med. Chem. Lett. 2014, 5, 979−982

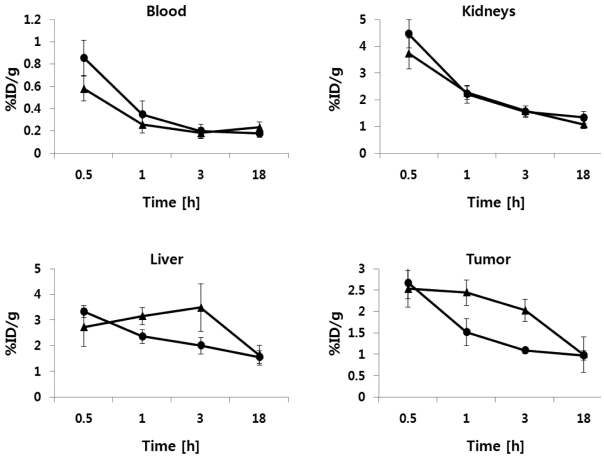

Figure 3. Comparison of biodistribution data of **3a** (●) and **3b** (▲) in nude mouse bearing U87MG tumors. Error bars denote the SDs (n = 4).

high liver-uptake by **3** can be explained by demetalation (^{64}Cu-dissociation from the chelate).[32,33] The degree of ^{64}Cu-demetalation from **3** is similar to that of other DOTA-based analogues.[34] It is not clear why **3b** shows slightly higher uptake than **3a**. The chelation effect of DO3A on ^{64}Cu demetalation is most apparent in the liver and lung (cf. Figure S1 compared with Tables S2 and S3, Supporting Information). For example, the %ID/g values for the free ^{64}Cu(II) ions reach 19 and 15 in the liver and lung, respectively (Figure S1, Supporting Information). The patterns for tumor-uptake of both complexes are similar. The uptake decreases as a function of time, with a slower excretion rate of **3b**, and the %ID/g values for each at selected time intervals are as follows: (1) 1.52 ± 0.31 (**3a**) and 2.44 ± 0.30 (**3b**) at 1 h p.i.; (2) 1.08 ± 0.06 (**3a**) and 2.02 ± 0.26 (**3b**) at 3 h p.i. These *in vivo* observations are in contrast to those observed *in vitro*, as previously described in the literature.[7]

The tumor regions of U87MG bearing mice are clearly visualized in the PET images (Figure 4). Of the three complexes employed, **3b** shows the highest tumor-uptake with %ID/g values as follows: 3.2 ± 0.8 (**3b**), 2.3 ± 1.5 (c(RGDyK)-DOTA-^{64}Cu), and 2 ± 0.5 (**3a**) (cf. Figure S2, Supporting Information). The blocking test demonstrates the

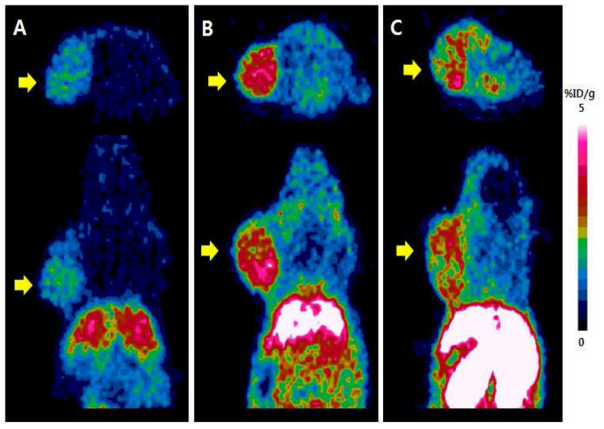

Figure 4. PET images of nude mice bearing U87MG tumor xenografts following injection of **3a** (A), **3b** (B), and c(RGDyK)-DOTA-^{64}Cu (C) at 1 h p.i. Tumors are indicated with arrows.

tumor specificity of **3** against $\alpha v\beta 3$ integrin receptors (Figure S3, Supporting Information). One feature of **3** is gallbladder enhancement, and **3b** shows a higher uptake rate in a given period of measurements (Figures S4 and S5, Supporting Information). As a result, hepatobiliary uptake followed by excretion through the intestine would be more predominant with **3b** than **3a** (Figure S4, Supporting Information). With **3a**, excretion is expected to occur primarily through the kidney. The binding affinities of **3a** and **3b** *in vitro* and *in vivo* are not exactly the same.

In conclusion, we have designed and synthesized two new bicyclic RGD peptides, c(RGD-ACP-K) (**1a**) and c(RGD-ACH-K) (**1b**), for use as bioconjugates with DO3A (**2a** and **2b**). Both complexes show high affinities toward U87MG glioblastoma cells, which are better than that of monocyclic c(RGDyK). The corresponding ^{64}Cu complexes (**3a** and **3b**) show high tumor uptake, as observed by PET, and **3b** exhibited a higher affinity than **3a**.

■ ASSOCIATED CONTENT

Ⓢ Supporting Information

Serum stabilities of **3a** and **3b** (Table S1), biodistribution results of **3a** (Table S2), **3b** (Table S3). and ^{64}Cu^{2+} (Figure S1), quantitative ROI analysis of **3a**, **3b**, and c(RGDyK)-DOTA-^{64}Cu (Figure S2), PET images of **3a** and **3b** with/without a blocking dose of c(RGDyK) (10 mg/kg) (Figure S3), and PET images of **3a** (Figure S4) and **3b** (Figure S5). This material is available free of charge via the Internet at http://pubs.acs.org.

■ AUTHOR INFORMATION

Corresponding Authors

*(J.Y.K.) E-mail: jykim@kirams.re.kr. Tel: +82-2-970-1464.
*(T-J.K.) E-mail: tjkim@knu.ac.kr. Tel: +82-53-950-4121.

Funding

This work was partially supported by the NRF (Grant No. 2011-0030161 and 2011-0030162).

Notes

The authors declare no competing financial interest.

■ ACKNOWLEDGMENTS

Anygen (Korea) is acknowledged for the synthesis of peptides and the MALDI-TOF measurements.

■ REFERENCES

(1) Hood, J. D.; Cheresh, D. A. Role of integrins in cell invasion and migration. *Nat. Rev. Cancer* **2002**, *2*, 91−100.

(2) Xiong, J. P.; Stehle, T.; Zhang, R.; Joachimiak, A.; Frech, M.; Goodman, S. L.; Arnaout, M. A. Crystal structure of the extracellular segment of integrin αVβ3 in complex with an Arg-Gly-Asp ligand. *Science* **2002**, *296*, 151−155.

(3) Fani, M.; Maecke, H. R.; Okarvi, S. M. Radiolabeled peptides: valuable tools for the detection and treatment of cancer. *Theranostics* **2012**, *2*, 481−501.

(4) Gaertner, F. C.; Kessler, H.; Wester, H. J.; Schwaiger, M.; Beer, A. J. Radiolabelled RGD peptides for imaging and therapy. *Eur. J. Nucl. Med. Mol. Imaging* **2012**, *39*, S126−138.

(5) Park, J. A.; Kim, J. Y. Recent advances in radiopharmaceutical application of matched-pair radiometals. *Curr. Top. Med. Chem.* **2013**, *13*, 458−469.

(6) Fani, M.; Maecke, H. R. Radiopharmaceutical development of radiolabelled peptides. *Eur. J. Nucl. Med. Mol. Imaging* **2012**, *39*, S11−30.

(7) Haubner, R. $\alpha_V\beta_3$-integrin imaging: a new approach to characterise angiogenesis? *Eur. J. Nucl. Med. Mol. Imaging* **2006**, *33*, S54−S63.
(8) Zhou, Y.; Chakraborty, S.; Liu, S. Radiolabeled cyclic RGD peptides as radiotracers for imaging tumors and thrombosis by SPECT. *Theranostics* **2011**, *1*, 58−82.
(9) Haubner, R.; Finsinger, D.; Kessler, H. Stereoisomeric peptide libraries and peptidomimetics for designing selective inhibitors of the $\alpha_v\beta_3$ integrin for a new cancer therapy. *Angew. Chem., Int. Ed.* **1997**, *36*, 1374−1389.
(10) Haubner, R.; Gratias, R.; Diefenbach, B.; Goodman, S. L.; Jonczyk, A.; Kessler, H. Structural and functional aspects of RGD-containing cyclic pentapeptides as highly potent and selective integrin $\alpha_V\beta_3$ antagonists. *J. Am. Chem. Soc.* **1996**, *118*, 7461−7472.
(11) Aumailley, M.; Gurrath, M.; Müller, G.; Calvete, J.; Timpl, R.; Kessler, H. Arg-Gly-Asp constrained within cyclic pentapeptides. Strong and selective inhibitors of cell adhesion to vitronectin and laminin fragment P1. *FEBS Lett.* **1991**, *291*, 50−54.
(12) Temming, K.; Schiffelers, R. M.; Molema, G.; Kok, R. J. RGD-based strategies for selective delivery of therapeutics and imaging agents to the tumour vasculature. *Drug Resist. Updates* **2005**, *8*, 381−402.
(13) Liu, S. Radiolabeled multimeric cyclic RGD peptides as integrin alphavbeta3 targeted radiotracers for tumor imaging. *Mol. Pharmaceutics* **2006**, *3*, 472−487.
(14) Liu, Z.; Shi, J.; Jia, B.; Yu, Z.; Liu, Y.; Zhao, H.; Li, F.; Tian, J.; Chen, X.; Liu, S.; Wang, F. Two ^{90}Y-labeled multimeric RGD peptides RGD4 and 3PRGD2 for integrin targeted radionuclide therapy. *Mol. Pharmaceutics* **2011**, *8*, 591−599.
(15) Li, Z. B.; Cai, W.; Cao, Q.; Chen, K.; Wu, Z.; He, L.; Chen, X. ^{64}Cu-labeled tetrameric and octameric RGD peptides for small-animal PET of tumor $\alpha_V\beta_3$ integrin expression. *J. Nucl. Med.* **2007**, *48*, 1162−1171.
(16) Li, Z. B.; Chen, K.; Chen, X. ^{68}Ga-labeled multimeric RGD peptides for microPET imaging of integrin $\alpha_V\beta_3$ expression. *Eur. J. Nucl. Med. Mol. Imaging* **2008**, *35*, 1100−1108.
(17) Hao, G.; Sun, X.; Do, Q. N.; Ocampo-Garcia, B.; Vilchis-Juarez, A.; Ferro-Flores, G.; De Leon-Rodriquez, L. M. Cyclization of RGD peptide sequences via the macrocyclic chelator DOTA for integrin imaging. *Dalton Trans.* **2012**, *41*, 14051−14054.
(18) Menichetti, L.; Kusmic, C.; Panetta, D.; Arosio, D.; Petroni, D.; Matteucci, M.; Salvadori, P. A.; Casagrande, C.; L'Abbate, A.; Manzoni, L. MicroPET/CT imaging of $\alpha_V\beta_3$ integrin via a novel ^{68}Ga-NOTA-RGD peptidomimet-ic conjugate in rat myocardial infarction. *Eur. J. Nucl. Med. Mol. Imaging* **2013**, *40*, 1265−1274.
(19) Manzoni, L.; Belvisi, L.; Arosio, D.; Bartolomeo, M. P.; Bianchi, A.; Brioschi, C.; Buonsanti, F.; Cabella, C.; Casagrande, C.; Civera, M.; De Matteo, M.; Fugazza, L.; Lattuada, L.; Maisano, F.; Miragoli, L.; Neira, C.; Pilkington-Miksa, M.; Scolastico, C. Synthesis of Gd and ^{68}Ga complexes in conjugation with a conformationally optimized RGD sequence as potential MRI and PET tumor-imaging probes. *ChemMedChem* **2012**, *7*, 1084−1093.
(20) Bianchini, F.; Cini, N.; Trabocchi, A.; Bottoncetti, A.; Raspanti, S.; Vanzi, E.; Menchi, G.; Guarna, A.; Pupi, A.; Calorini, L. ^{125}I-radiolabeled morpholine-containing argine-glycine-aspartate (RGD) ligand of $\alpha_V\beta_3$ integrin as a molecular imaging probe for angiogenesis. *J. Med. Chem.* **2012**, *55*, 5024−5033.
(21) Casiraghi, G.; Rassu, G.; Auzzas, L.; Burreddu, P.; Gaetani, E.; Battistini, L.; Zanardi, F.; Curti, C.; Nicastro, G.; Belvisi, L.; Motto, I.; Castorina, M.; Giannini, G.; Pisano, C. Grafting aminocyclopentane carboxylic acids onto the RGD tripeptide sequence generates low nanomolar $\alpha_V\beta_3/\alpha_V\beta_5$ integrin dual binders. *J. Med. Chem.* **2005**, *48*, 7675−7687.
(22) Auzzas, L.; Zanardi, F.; Battistini, L.; Burreddu, P.; Carta, P.; Rassu, G.; Curti, C.; Carsiraghi, G. Targeting $\alpha_V\beta_3$ integrin: design and applications of mono- and multifunctional RGD-based peptides and semipeptids. *Curr. Med. Chem.* **2010**, *17*, 1255−1299.
(23) Kim, J. Y.; Park, H.; Lee, J. C.; Kim, K. M.; Lee, K. C.; Ha, H. J.; Choi, T. H.; An, G. I.; Chen, G. J. A simple Cu-64 production and its application of Cu-64 ATSM. *Appl. Radiat. Isot.* **2009**, *67*, 1190−1194.
(24) Haubner, R.; Kuhnast, B.; Mang, C.; Weber, W. A.; Kessler, H.; Wster, H. J.; Schwaiger, M. [^{18}F]Galacto-RGD: synthesis, radio-labeling, metabolic stability, and Radiation dose estimates. *Bioconjugate Chem.* **2004**, *15*, 61−69.
(25) Shetty, D.; Jeong, J. M.; Kim, Y. J.; Lee, J. Y.; Hoigebazar, L.; Lee, Y. S.; Lee, D. S.; Chung, J. K. Development of a bifunctional chelating agent containing isothiocyanate residue for one step F-18 labeling of peptides and application for RGD labeling. *Bioorg. Med. Chem.* **2012**, *20*, 5941−5947.
(26) Deristoforo, C.; Gonzalez, I. H.; Carlsen, J.; Rupprich, M.; Huisman, M.; Virgolini, I.; Wester, H. J.; Haubner, R. ^{68}Ga- and ^{111}In-labelled DOTA-RGD peptides for imaging of $\alpha v\beta 3$ intergrin expression. *Eur. J. Nucl. Med. Imaging* **2008**, *35*, 1507−1515.
(27) Knetsch, P. A.; Petrik, M.; Griessinger, C. M.; Rangger, C.; Fani, M.; Kesenheimer, C.; Guggenberg, E.; Pichler, B. J.; Virgolini, I.; Desritoforo, C.; Haubner, R. [^{68}Ga] NODAGA-RGD for imaging $\alpha v\beta_3$ intergrin expression. *Eur. J. Nucl. Med. Mol. Imaging* **2011**, *38*, 1303−1312.
(28) De León-Rodríguez, L. M.; Zoltan, K. The synthesis and chelation chemistry of DOTA− peptide conjugates. *Bioconjugate Chem.* **2008**, *19*, 391−402.
(29) McMurry, J. Organic Compounds: Alkanes and Cycloalkanes. In *Organic Chemistry*, 6th ed.; Brooks/Cole-Thomson Learning: Belmont, CA, 2004; pp 88−92.
(30) Schelstraete, K.; De Vis, K.; Vermeulen, F. L.; Deman, J.; Sambre, J.; Goethals, P.; Van Haver, D.; Slegers, G.; Vandecasteele, C.; De Schryver, A. Uptake of ^{11}C-aminocyclopentane carboxylic acid (ACPC) and ^{13}N-ammonia in malignant tumors a comparative clinical study. *Nuclear Medicine in Clinical Oncology*; Springer Berline Heidelberg. 1986; pp 250−253.
(31) McConathy, J.; Goodman, M. M. Non-natural amino acids for tumor imaging using positron emission tomography and single photon emission computed tomography. *Cancer Metastasis Rev.* **2008**, *27*, 555−573.
(32) Chen, X.; Hou, Y.; Tohme, M.; Park, R.; Khankaldyyan, V.; Gonzales-Gomez, I.; Bading, J. R.; Laug, W. E.; Conti, P. S. Pegylaed Arg-Gly-Asp peptide: ^{64}Cu labeling and PET imaging of brain tumor $\alpha_V\beta_3$-integrin expression. *J. Nucl. Med.* **2004**, *45*, 1776−1783.
(33) Woodin, K. S.; Heroux, K. J.; Boswell, C. A.; Wong, E. H.; Weisman, G. R.; Niu, W.; Tomellini, S. A.; Anderson, C. J.; Zakharov, L. N.; Rheingold, A. L. Kinetic inertness and electrochemical behavior of copper (II) tetraazamacrocyclic complexes: Possible implications for in vivo stability. *Eur. J. Inorg. Chem.* **2005**, *23*, 4829−4833.
(34) Dumont, R. A.; Deininger, F.; Haubner, R.; Maecke, H. R.; Weber, W. A.; Fani, M. Novel ^{64}Cu and ^{64}Ga-labeled RGD conjugates show improved PET imaging of $\alpha_v\beta_3$ integrin expression and facile radiosynthesis. *J. Nucl. Med.* **2011**, *52*, 1276−1284.